UDC 539.4

# A Probabilistic Model for Describing Short Fatigue Crack Growth Behavior of LZ50 Steel

**B. Yang,[1] B. Q. Ma, S. N. Xiao, and Y. X. Zhao**

State Key Laboratory of Traction Power, Southwest Jiaotong University, Chengdu, China

[1] yb@swjtu.cn

*Fatigue damage process of metal components and structures with smooth surface belongs primarily to stage of short fatigue crack. To characterize the random growth behavior of short fatigue crack and to apply the crack growth rate model for engineering safety assessment, a probabilistic model is proposed with consideration of the test data scattering regularity. This probabilistic model is based on the multi-microstructural barriers model and can describe the deceleration behavior of growth rate during the whole short fatigue crack propagation process. To take the statistical characteristics of whole test data into account, the idea from the general maximum likelihood method which is widely used in parameters estimation of fatigue* $S-N$ *curves and* $\varepsilon-N$ *curves is inherited. While estimating the parameters of the probabilistic model, conventional correlation coefficient optimization method is extended for calculating the parameters of both the mean curve and the standard deviation curve. Analysis on the test data of LZ50 steel indicates the reasonability and availability of present model.*

***Keywords***: short fatigue crack, probabilistic model, parameters estimation, LZ50 steel.

**Introduction**. With the increase of speed, transport capacity and traffic density of railway vehicles in China, service conditions for key structures of vehicles are harsher than before [1]. Axle is an important component for vehicle running gear. It bears complicated alternate loadings during operation, and is the component with the highest loading frequency and the most complex failure modes [2]. If the failure of axle caused by fatigue damage gets out of controllable, vehicles are likely to derail, and the safety of railway operation will be gravely affected. The fatigue failure of structures and components with smooth surface under cyclic loads is subject to the initiation and propagation of short fatigue cracks (SFCs). This process can account for more than 70% of the total fatigue life for a majority of metal components and structures with smooth surface [3]. For example, with an overhaul cycle of 100,000 km and a survival reliability of 0.999, the critical size of semi-elliptical crack on the load relieving groove of RD2 axle is 1.23 mm, and the size of circumferential crack is only 0.94 mm [4, 5]. Therefore it is obvious that the fatigue damage process of axle belongs primarily to SFC scope.

To depict the SFC growth behavior, many researches have been carried out. Accordingly, a lot of SFC growth rate models have been proposed, such as the cyclic stress or strain related model [6, 7], the shearing strain model [8], the dislocation based model [9], the general Paris law model [10], and the effective SFC model [11]. However, the scatter of fatigue test data is an intrinsic fatigue phenomenon of engineering materials [12, 13]. To utilize the SFC growth model for safety estimation and fatigue damage tolerance design of engineering structures, it is necessary to develop its probabilistic model.

LZ50 steel is one of the widely utilized axle materials which is applied for Chinese speed increased and heavy haul freight cars. Present study is based on previous replica tests of this material. The scattering property of test data is considered by developing the probabilistic form of the multi-microstructural barriers model [14]. Parameters estimation method, which is an extension of conventional correlation coefficient optimization method [15], is introduced in detail.

## 1. **Experiments and Brief Introduction of Multi-Microstructural Barriers Model**.

1.1. ***Materials, Specimens, and Replica Tests***. Test material of present work is LZ50 axle steel, which is widely used in Chinese railway industry. It is a kind of the medium carbon steel and the chemical composition was introduced clearly in reference [14]. The statistical mechanical properties at room temperature are: 209750 MPa for the Young modulus, 656.43 MPa for tensile strength, 383.57 MPa for yield strength, 54.71% for elongation, and 26.57% for cross-sectional area reduction [14]. Two main microstructural barriers exist in present material, i.e., ferrite grain boundary and rich pearlite band structure. The mean value of equivalent diameters, $d_1$, for ferrite grain is 14.61 $\mu$m while that of the interval, $d_2$, between two rich pearlite bands is 109.09 $\mu$m. The standard deviations of them are 1.40 and 9.28 $\mu$m, respectively. It is clear that a great microstructural dispersion exists in the material. The static hardness of microstructure for ferrite of the steel is 191.4 HV0.1, while that for pearlite is 223.4 HV0.1. To study the SFC growth behavior of present material, totally 7 smooth axial hourglass shaped specimens with 10 mm diameter were processed.

Replica tests were carried out on Rumul 250 kN high frequency fatigue test machine under a stress-controlled sine wave mode. The stress amplitude was 230 MPa with a stress ratio of $-1$. Tests were suspended at given cycle number intervals while a tensile stress of 10 MPa was maintained for replicating the specimen surface. To study the relationship between cracks and microstructures, specimen surfaces were etched by 4% nitric acid alcohol and the metallographic structure was exposed. The replica film and the solvent were acetyl cellulose film and acetone respectively. For each specimen, total replicating times is more than 12 while the average fatigue life of all the 7 specimens is 137,707 cycles [14]. Dried replicas were flattened by two glass slides before being observed using an auto-montage micro-observation system. To facilitate finding the SFCs, an inverted sequence method suggested in reference [11] was applied after the tests.

1.2. ***Multi-Microstructural Barriers Model***. Based on the replica test data, a multi-microstructural barriers model was proposed by Yang et al [14]. This model followed the effective SFC criterion, and included the characteristic sizes of the material microstructures, $d_1$ and $d_2$. In addition, a resistance coefficient function was proposed to depict the periodical influence of microstructural barriers on SFC growth. The multi-microstructural barriers model can be defined as

$$\frac{da}{dN} = G_0 + A[\Delta W_t a - \Delta W_t \sum_{i=1}^{n} f_i(\Delta d_i) d_i]^m, \tag{1}$$

where $a$ is dominant short crack (DSC) size, $N$ is cyclic number, $G_0$ is the lowest growth rate in the scope of the first microstructural barrier range, $\Delta W_t$ is the total cyclic strain energy density of remote fields, which can be estimated by utilizing the cyclic constitutive equation, $d_i$ is the characteristic microstructural barrier size, $i$ is the subscript to clarify the kinds of barriers, i.e., $d_1$ for average equivalent diameter of ferrite grains and $d_2$ for mean value of intervals between two rich pearlite bands, $A$ and $m$ are corresponding material constants, $f_i(\Delta d_i)$ is the resistance coefficient function and is defined as

$$f_i(\Delta d_i) = 1 - \left(\frac{d_i - \Delta d_i}{d_i}\right)^{\alpha_i}, \tag{2}$$

where $\Delta d_i$ is the distance between dominant short crack tip and the boundary of previous microstructure and $d_i - \Delta d_i$ is the distance between the dominant short crack tip and the next microstructural barrier. This resistance coefficient function indicates that the closer the dominant short crack tip is to barrier, the stronger the constraint force is.

Fitting effect of the multi-microstructural barriers model to test data of single specimen is shown in Fig. 1. It can be seen that the prediction curve has a good fitting effect to test data. In addition, it illustrates the periodical effect of main microstructural barriers on SFC growth behavior [14].

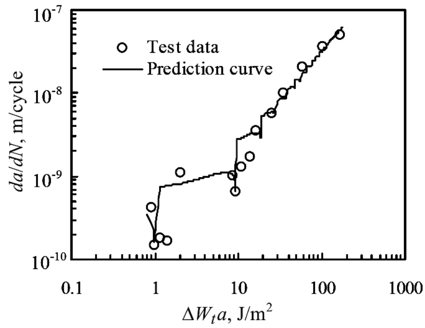


Fig. 1. SFC growth rate curve for a typical specimen of LZ50 steel [14].

2. **Probabilistic Fatigue Short Crack Growth Rate Model**. Due to the intrinsic scatter of fatigue test data obtained from different specimens as shown in Fig. 2, it's necessary to construct probabilistic model to make it possible for safety estimation and fatigue damage tolerance design of in-service structures. As shown in Table 1, in terms of statistic, the average DSC sizes are 14.77 and 107.11 $\mu$m, respectively, when the first and the second deceleration happen. It is worth noting that these two values are very close to the statistical sizes of microstructural barriers, $d_1$ and $d_2$, mentioned in Sect. 1.1. From this, it can be proved that the DSC growth deceleration is due to the constraints of microstructural barriers.

Table 1

**Data of DSC Sizes when Two Decelerations Happen and Corresponding Basic Statistical Parameters**

| Deceleration | DSC sizes of different specimens ($\mu$m) | | | | | | | Statistical parameters ($\mu$m) | |
|---|---|---|---|---|---|---|---|---|---|
| | 1 | 2 | 3 | 4 | 5 | 6 | 7 | Mean value | Standard deviation |
| 1st time | 12.16 | 17.78 | 14.88 | 16.05 | 14.51 | 11.48 | 16.55 | 14.77 | 2.29 |
| 2nd time | 116.8 | 99.86 | 86.75 | 121.5 | 122.1 | 93.63 | 109.2 | 107.1 | 14.01 |

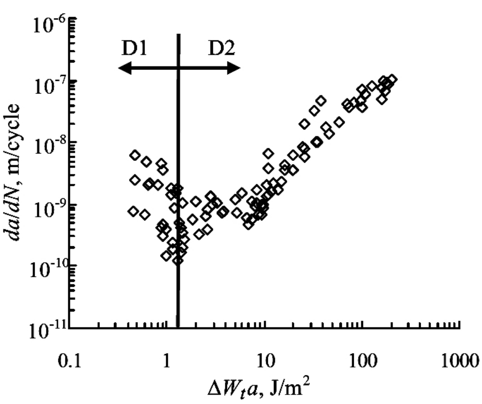


Fig. 2. Test data of 7 specimens of LZ50 steel.

2.1. ***Probabilistic Form of Short Fatigue Crack Growth Rate Model***. Based on the multi-microstructural barriers model, it can be rewritten by taking logarithm to the both sides of Eq. (1) as

$$\log\left(\frac{da}{dN}-G_0\right)=\log A+m\log\left\{\left[\Delta W_t a-\Delta W_t\sum_{i=1}^{n} f_i(\Delta d_i)d_i\right]\right\}. \quad (3)$$

It can be linearized as

$$Y=A'+B'X, \quad (4)$$

where

$$\log(da/dN-G_0)=Y,\quad \log\left\{\left[\Delta W_t a-\Delta W_t\sum_{i=1}^{n} f_i(\Delta d_i)d_i\right]\right\}=X,\quad \log A=A',\quad m=B'.$$

Previous research has discovered that with given stress intensity factor, crack growth rate obeys logarithmic normal distribution (LND) [16]. Assuming that the material constants, which are random variables to be solved based on test data, are at the same probabilistic level and considering the scattering character of test data, the statistical property of random SFC growth rate following LND can be described by two equations, i.e., the mean curve equation and the standard deviation curve equation

$$Y_{av}=A'_{av}+B'_{av}X, \quad (5)$$

$$Y_s=A'_s+B'_sX, \quad (6)$$

where subscripts *av* and *s* indicate the mean value and the standard deviation value, separately.

For any equation obeying LND and under any given survival probability of $P$, the crack growth rate $Y_P$ can be given by

$$Y_P=Y_{av}+Z_PY_s, \quad (7)$$

where $Z_P$ is the percentage of normal distribution with a probability of $P$. Then by introducing Eq. (5) and (6), Eq. (7) can be written as

$$Y_P=A'_{av}+B'_{av}X+Z_P(A'_s+B'_sX)=(A'_{av}+Z_PA'_s)+(B'_{av}+Z_PB'_s)X. \quad (8)$$

It can be simplified as

$$Y_P=A'_P+B'_PX. \quad (9)$$

2.2. ***Parameters Estimation of Probabilistic Model***.

2.2.1. *Mean Curve*. It can be seen from Eq. (4) that $Y$ correlates linearly with $X$. To consider the statistical properties of all the test data, the idea from the general maximum likelihood method [17] which is extensively applied in fatigue curve parameters estimation is inherited while estimating the parameters of the probabilistic model. That is, test data obtained from different specimens is applied all together to obtain corresponding probabilistic parameters. Hence, using the conventional correlation coefficient optimization method [15], $A'_{av}$ and $B'_{av}$ can be calculated by

$$A'_{av} = \overline{Y} - B'_{av}\overline{X}, \tag{10}$$

$$B'_{av} = \frac{L_{XY}}{L_{XX}}, \tag{11}$$

where

$$\overline{Y} = \frac{1}{k}\sum_{i=1}^{k} Y_i, \tag{12}$$

$$\overline{X} = \frac{1}{k}\sum_{i=1}^{k} X_i, \tag{13}$$

$$L_{XX} = \sum_{i=1}^{k}(X_i^2) - \frac{1}{k}\left(\sum_{i=1}^{k} X_i\right)^2, \tag{14}$$

$$L_{XY} = \sum_{i=1}^{k}(X_i Y_i) - \frac{1}{k}\left(\sum_{i=1}^{k} X_i\right)\left(\sum_{i=1}^{k} Y_i\right), \tag{15}$$

where $k$ is the total number of test data, $(da/dN,\ \Delta W_t a)$, for all the 7 specimens.

Values of $\overline{X}$, $L_{XX}$, and $L_{XY}$ are all linked to $X$, the determination of which is relevant to the resistance coefficient function. So the parameter $\alpha_i$ in $f_i(\Delta d_i)$ should be estimated in advance. For present material, that means $\alpha_1$ in resistance coefficient function for ferrite grain boundary and $\alpha_2$ in resistance coefficient function for rich pearlite bands are to be determined in advance. According to the theory of least square method, $\alpha_1$ and $\alpha_2$ should make the absolute value of fitting correlation coefficient $R_{XY}$ to be as closer to 1 as possible. The definition of $R_{XY}$ is

$$R_{XY} = \frac{L_{XY}}{\sqrt{L_{XX} L_{YY}}}. \tag{16}$$

By searching $\alpha_1$ and $\alpha_2$ in their value range $(0 \le \alpha_1 \le 1,\ 0 \le \alpha_2 \le 1)$, the maximum value of $R_{XY}$ can be determined. Thereby, $A'_{av}$ and $B'_{av}$ are calculable by Eqs. (10) and (11).

2.2.2. *Standard Deviation Curve*. By extending the conventional correlation coefficient optimization method with utilization of the whole test data, the way present work evaluates parameters of standard deviation curve is quite different from other methods.

As is well-known, the standard deviation is a statistical value that indicates the scattering characteristics of data. It's also a constant positive index which can reflects the scattering extent by taking the deviation between mean value and observed value into account [18]. Similarly, the standard deviation curve should be a curve which can reflect the deviation extent of observed value comparing to the mean curve. Thus, it is suitable and practicable to evaluate curve parameters in Eq. (6) by fitting all $\Delta W_t a_i$ with relevant absolute values of growth rate deviation, $|\delta_i|$. Definition of $\delta_i$ is

$$\delta_i = \log\left(\frac{da}{dN} - G_0\right)_i - Y_{av}(\Delta W_t a_i). \tag{17}$$

Values of $A_s'$ and $B_s'$ can be determined by

$$A_s' = \overline{Y} - B_s'\overline{X}, \tag{18}$$

$$B_s' = \frac{L_{XY}}{L_{XX}}. \tag{19}$$

It should be noted that during the parameters estimation process of standard deviation curve, $Y_i$ is no longer $\log(da/dN - G_0)_i$. It's the absolute value of growth rate deviation, $|\delta_i|$.

Considering that $\alpha_1$ and $\alpha_2$ are parameters related to the kinds of microstructural barriers, once they are determined for the mean curve, they should remain the same for both the standard deviation curve and the probabilistic curve. Therefore, the same values of $\alpha_1$ and $\alpha_2$ are utilized for calculating material constants $A_s'$ and $B_s'$.

2.2.3. *Probabilistic Curve*. After obtaining the parameters of both mean curve and standard deviation curve, probabilistic parameters for short crack growth rate curve with given survival probability $P$ as shown in Eq. (8) can be calculated by following two equations:

$$A_P' = A_{av}' + Z_P A_s', \tag{20}$$

$$B_P' = B_{av}' + Z_P B_s'. \tag{21}$$

Finally, according to the relation, $A_P = 10^{A'}$ and $m_P = B'$, the probabilistic description of Eq. (1) can be expressed as

$$\left(\frac{da}{dN}\right)_P = G_0 + A_P\left[\Delta W_t a - \Delta W_t \sum_{i=1}^{n} f_i(\Delta d_i) d_i\right]^{m_P}. \tag{22}$$

3. **Example of Probabilistic Curve for LZ50 Steel**. To indicate the reasonability and the validity of the proposed probabilistic SFC growth rate model, parameters estimation were performed and fitting effects were illustrated for LZ50 steel.

Previous research [14] has proved that before DSC firstly breaks the ferrite grain boundary, this boundary is the dominant microstructural barrier which contributes most for restricting crack growth. Once it is broken through, the dominant microstructural barrier becomes the rich pearlite band structure. As shown in Fig. 2, difference of distribution trend is significant between test data before (stage *D1*) and after (stage *D2*) the dominant short crack firstly breaking through the ferrite boundary barrier. To avoid this difference influencing the fitting effect and also to facilitate solving the statistical parameters and emphasizing the role of dominant microstructural barrier in stage *D1* and *D2*, following calculation steps were suggested:

*Step 1*. Set a dividing line parallel to vertical coordinate at the data point of lowest crack growth rate as shown in Fig. 2. Thus the whole data can be separated in two groups in accordance with stage *D1* and *D2*.

*Step 2*. Process data in stage *D2* by utilizing method introduced in Sect. 2.2 so as to obtain the parameters of probabilistic crack growth curve after the first significant deceleration of crack growth rate.

*Step 3*. The parameters $\alpha_1$ and $\alpha_2$ of the resistance coefficient function should be kept the same as the values obtained in step 2, and then process data in stage *D1* to determine the parameters of probabilistic curve before the first significant deceleration of crack growth rate.

According to above three calculation steps, the basic probabilistic curve parameters of LZ50 steel can be obtained:

(i) general parameters: $G_0 = 1.21 \cdot 10^{-10}$ m/cycle, $d_1 = 8.03 \cdot 10^{-6}$ m, $d_2 = 5.36 \cdot 10^{-5}$ m, $\alpha_1 = 0.27$, $\alpha_2 = 0.16$;

(ii) parameters for curve in stage *D1*: $A'_{av} = -8.6458$, $B'_{av} = 1.1321$, $A'_s = 0.6244$, $B'_s = 0.1014$;

(iii) parameters for curve in stage *D2*: $A'_{av} = -9.8239$, $B'_{av} = 1.2094$, $A'_s = 0.3802$, $B'_s = 0.13$.

Thereby, parameters for probabilistic curves with typical survival probabilities can be listed in Table 2. Fitting effect of probabilistic SFC rate model to test data is depicted in Fig. 3. It can be seen that the probabilistic curves illustrate the change of test data effectively and can reflect the periodical fluctuation of growth rate. When the value of $\Delta W_t a$ is given, the higher the probability $P$ is, the faster the SFC propagates.

Table 2

**Parameters for Probabilistic SFC Growth Rate Curves with Typical Survival Probabilities**

| $P$ | Data in stage *D1* | | | | Data in stage *D2* | | | |
|---|---|---|---|---|---|---|---|---|
| | $A'_P$ | $B'_P$ | $A$ | $m$ | $A'_P$ | $B'_P$ | $A$ | $m$ |
| 0.5 | −8.6458 | 1.1321 | $2.26 \cdot 10^{-9}$ | 1.1321 | −9.8239 | 1.2094 | $1.50 \cdot 10^{-10}$ | 1.2094 |
| 0.9 | −7.8456 | 1.2621 | $1.43 \cdot 10^{-8}$ | 1.2621 | −9.3366 | 1.0429 | $4.61 \cdot 10^{-10}$ | 1.0429 |
| 0.95 | −7.6188 | 1.2989 | $2.41 \cdot 10^{-8}$ | 1.2989 | −9.1985 | 0.9956 | $6.33 \cdot 10^{-10}$ | 0.9956 |
| 0.99 | −7.1933 | 1.3681 | $6.41 \cdot 10^{-8}$ | 1.3681 | −8.9394 | 0.9071 | $1.15 \cdot 10^{-9}$ | 0.9071 |
| 0.999 | −6.7164 | 1.4456 | $1.92 \cdot 10^{-7}$ | 1.4456 | −8.6489 | 0.8078 | $2.24 \cdot 10^{-9}$ | 0.8078 |
| 0.1 | −9.4460 | 1.0021 | $3.58 \cdot 10^{-10}$ | 1.0021 | −10.311 | 1.3759 | $4.88 \cdot 10^{-11}$ | 1.3759 |
| 0.05 | −9.6728 | 0.9652 | $2.12 \cdot 10^{-10}$ | 0.9652 | −10.449 | 1.4232 | $3.55 \cdot 10^{-11}$ | 1.4232 |
| 0.01 | −10.098 | 0.8961 | $7.97 \cdot 10^{-11}$ | 0.8961 | −10.708 | 1.5117 | $1.96 \cdot 10^{-11}$ | 1.5117 |
| 0.001 | −10.575 | 0.8186 | $2.66 \cdot 10^{-11}$ | 0.8186 | −10.999 | 1.6110 | $1.00 \cdot 10^{-11}$ | 1.6110 |

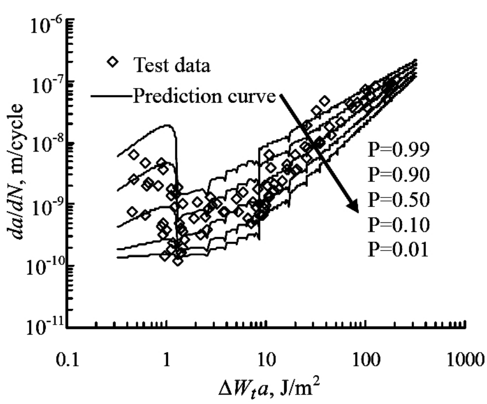


Fig. 3. Typical probabilistic SFC growth rate curves of LZ50 steel.

**Conclusions**. A probabilistic SFC growth rate model is proposed based on the multi-microstructural barriers model. It can describe the statistical properties of test data adequately. During the parameters estimation process for probabilistic curves, the correlation coefficient optimization method is applied and extended effectively. Fitting and analysis on the test data of LZ50 steel illustrates the accuracy and applicability of the proposed model.

***Acknowledgments***. Present work is supported by the National Natural Science Foundation of China (51205326 and 51275432), the Opening Project of State Key Laboratory of Traction Power (Grant No. 2015TPL_T13), and the Fundamental Research Funds for the Central Universities (SWJTU11CX075).

1. Z. Y. Shen, Y. X. Zhao, B. Yang, and J. C. Peng, "Progresses on the fatigue reliability research of China railway," *Adv. Mater. Res.*, **44-46**, 1–4 (2008).
2. Y. X. Zhao, Q. Gao, B. Zhang, and K. J. Diao, "Key solid mechanics issues and research progresses for railway vehicle wheelset," *Chin. J. Solid Mech.*, **31**, No. 6, 716–730 (2010).
3. K. J. Miller, "The behaviour of short fatigue cracks and their initiation. Part II-A. General summary," *Fatigue Fract. Eng. Mater. Struct.*, **10**, 93–113 (1987).
4. Y. X. Zhao, B. Yang, and M. F. Feng, "Critical safety fatigue crack sizes for the RD2 type axle of Chinese railway freight car," in: S. J. Wu, P. E. J. Flewitt, and Z. Zhang (Eds.), Proc. 9th Int. Conf. on *Engineering Structural Integrity Assessment* (Beijing, China, 2007), China Machine Press (2007), pp. 1194–1199.
5. Y. X. Zhao, B. Yang, M. F. Feng, et al., "Probabilistic critical fatigue safety state of the RD2 type axle of China railway freight car," *Adv. Mater. Res.*, **44-46**, 751–758 (2008).
6. M. W. Brown, "Interfaces between short, long and non-propagating cracks," in: K. J. Miller and E. R. de los Rios (Eds.), *The Behaviour of Short Fatigue Cracks*, Mechanical Engineering Publications, London (1986), pp. 423–439.
7. P. D. Hobson, M. W. Brown, and E. R. de los Rios, "Two phases of short crack growth in a medium carbon steel," in: K. J. Miller and E. R. de los Rios (Eds.), *The Behaviour of Short Fatigue Cracks*, Mechanical Engineering Publications, London (1986), pp. 441–459.
8. K. J. Miller, H. J. Mohamed, and E. R. de los Rios, "Barriers to short fatigue crack propagation at low stress amplitude in a banded ferrite-pearlite structure," in: R. O. Ritchie and J. A. Lankford (Eds.), *Small Fatigue Cracks*, Metallurgical Society of AIME, Warrendale, PA (1986), pp. 639–656.
9. A. Navarro and E. R. de los Rios, "A model for short fatigue crack propagation with an interpretation of the short-long crack transition," *Fatigue Fract. Eng. Mater. Struct.*, **10**, 169–186 (1987).
10. J. Polak J and P. Liskutin, "Nucleation and short crack growth in fatigued polycrystalline copper," *Fatigue Fract. Eng. Mater. Struct.*, **13**, 119–133 (1990).
11. Y. X. Zhao, Q. Gao, and J. N. Wang, "Interaction and evolution of short fatigue cracks," *Fatigue Fract. Eng. Mater. Struct.*, **22**, 459–468 (1999).
12. Y. X. Zhao, J. N. Wang, and Q. Gao, "Random cyclic stress-strain responses of a stainless steel pipe-weld metal I – A statistical investigation," *Nucl. Eng. Des.*, **199**, 303–314 (2000).
13. Y. X. Zhao, Q. Gao, and J. N. Wang, "Random cyclic stress-strain responses of a stainless steel pipe-weld metal II – A modeling," *Nucl. Eng. Des.*, **199**, 315–326 (2000).
14. B. Yang and Y. X. Zhao, "Experimental research on dominant effective short fatigue crack behaviour for railway LZ50 axle steel," *Int. J. Fatigue*, **35**, 71–78 (2012).

15. Z. T. Gao and J. J. Xiong, *Fatigue Reliability*, BUAA Press, Beijing (2000).

16. M. Liao, N. Tang, and Q. X. Yang, "A statistical investigation of fatigue crack initiation and growth process based upon a large sample size experiment," *Acta Mech. Solida Sinica*, **17**, 1–10 (1996).

17. Y. X. Zhao, Q. Gao, and J. N. Wang, "Unified approach for estimating the probabilistic design *S–N* curves of three commonly used fatigue stress-life models," *Nucl. Power Eng.*, **22**, 42–52 (2001).

18. B. Yang and Y. X. Zhao, "A new method for parameters estimation of probabilistic fatigue crack growth rate model," *Key Eng. Mater.*, **324-325**, 615–618 (2006).

Received 03. 08. 2015